

# Dynamic processes happening during the evaporation of films of fusible materials

L N Orlikov<sup>1</sup>, N L Orlikov<sup>2</sup>, S A Ghyngazov<sup>2</sup> and S M Shandarov<sup>1</sup>

<sup>1</sup>The Chair of Electronic Devices, Tomsk State University of Control Systems and Radioelectronics, 40 Lenin Ave, 634050, Tomsk, Russia

<sup>2</sup>Tomsk Polytechnic University, 30 Lenin Ave, 634050, Tomsk, Russia

E-mail: [oln4@yandex.ru](mailto:oln4@yandex.ru)

**Abstract.** The formation of optically-transparent films of fusible materials like zinc, lead, bismuth on glass substrates to obtain single-mode optical diffusive waveguides is considered. The quality of films for waveguides depends on the amount of oxygen in residual environment, the gas exchange rate in the working chamber, the rate of oxygen desorption from the heated elements in vacuum chamber, the evaporator and the substrate. The regularities of variations of local layer thickness and the procedure phase diagram from the local gas exchange rate are determined.

## 1. Introduction

Optical waveguides on glass substrates are a promising area in their application in simple and cheap optoelectronic devices. As shown in [1], the highest refractive index is achieved during the formation of waveguides by oxidized film diffusion. However, realization of a number of electro-optical effects is restrained by probabilistic repeatability of wave guiding layers which holds down the development of optoelectronics [1-3]. This happens due to the fact that film formation in gas exchange mode isn't explored enough. One of the reasons of probabilistic repeatability of local thickness and film composition is dynamic processes which happen during the material evaporation. The regularities of evaporation, which were earlier found by Knudsen, Langmuir and other scientists for point sources, fail when it comes to the line where one material escape into another state. Most materials, which have three states – solid, liquid, gaseous – at ambient pressure heating, in vacuum, lose their liquid state partly or completely. Moreover, the film distribution over the substrate is quite unclear because of the poor study of molecular vapor flow and substrate interaction.

## 2. Methodology

One of the ways to solve the stated problem is to analyze the structure of molecular flow and to apply the regularities of vapor flow and material-substrate interaction [4-8].

## 3. Simulation of vapor flow formation

We know several models of gas and vapor formation.

Knudsen model (fig. 1a). Knudsen flow suggests spherical free molecule flow from the point source without taking into account the interaction with the substrate. Herewith, it is the realization of the cosine law of film distribution over the substrate with mass transfer which is inversely proportional



to the squared distance to the substrate. Some works [2, 5] introduce evaporation and condensation probability functions.

Hydrodynamic model (fig. 1b, c). The 1990s witnessed the development of gas and vapor formation model in the approximation of Navier–Stokes equations [6-8]. Below are some of its statements.

We know that the evaporation temperature is the temperature at which vapor pressure tends to 1 Pa. During the formation of films, the pressure in vacuum chamber is held at the value of about 0,01 Pa and lower to provide the molecule transition to the substrate and minimal interactions of residual gas with metal vapor. As a result, the vapor flow is overlapped by pressure difference by the 2-3 orders and more. The flow shape, temperature, pressure, extension angle and flow rate are defined by the functions [6] which depend on the ratio of evaporation pressure (about 1 Pa) to ambient pressure ( $\sim 0,1-0,01$  Pa). The flow effusion can change from the shape of torch to the shape of sphere.

Figure 1a shows the conditional distribution of complete film coating thickness in accordance with Knudsen model and Hydrodynamic model (fig. 1b, c). Figure 2 shows the functions of gas flow temperature and pressure distribution [6].

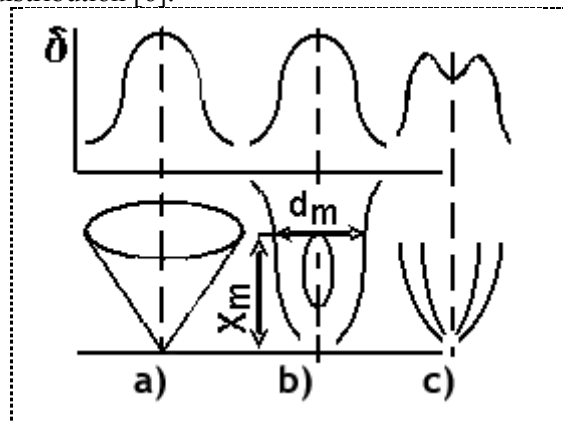


**Figure 1.** Film distribution over the substrate: a) according to Knudsen model; b), c) according to hydrodynamic model.

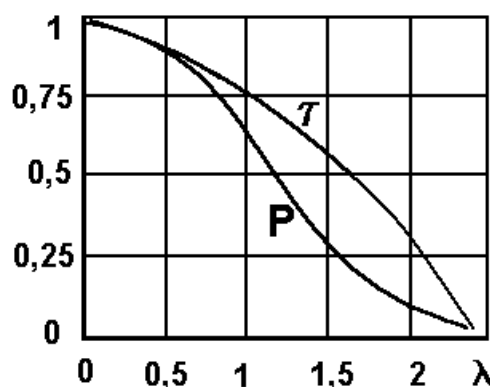


**Figure 2.** Flow parameters function.

The main characteristic of the flow is the rate coefficient  $\lambda = V/V'$ , which is equal to ratio of flow particle velocity to the effusion cutoff velocity. When  $\lambda=0$ , the flow is static; when  $\lambda=1$ , the flow achieves the sound velocity; when  $\lambda>1$ , the speed is supersonic. The speed of temperature change is defined by the equation:

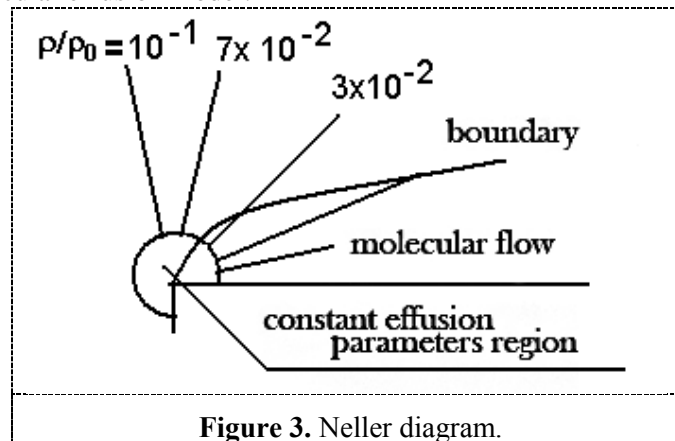
$$\tau(\lambda) = T/T^* = [1 - (k-1)/(k+1)\lambda^2] \quad (1)$$

The equation of the full pressure change is:

$$\pi(\lambda) = P/P^* = [1 - (k-1)/(k+1)\lambda^2]^{k/(k-1)}, \quad (2)$$

where  $k=1,3$  is adiabatic exponent of hot vapor.

Figure 3 shows Neller diagram [9], which demonstrates that at small densities the flow is formed in accordance with molecular effusion model.



#### 4. Experimental studies

Visualization of lead vapor flow in magnetron discharge plasma [10] showed that the vapor flow from the crucible to substrate gets the shape of sphere at the chamber pressures (0,1 - 0,01 Pa). When the chamber pressure is more than 0,1 Pa the flow gets the shape of several torches (cycles). It happens in accordance with Neller diagram. The transversal and longitudinal dimensions of the first expansion cycle ( $d_m$  и  $X_m$ ), after which the film thickness variation is less than 2%, follow the laws of gas flow dynamics [6] and depend on the ratio of evaporation pressure ( $P_j \sim 1$  Pa) to the pressure  $P_k$  in vacuum chamber ( $P_j / P_k$ ).

$$X_m = (0,7 - 1,34)d(kP_j / P_k)^{0,5} \quad (3)$$

$$d_m = d(kP_j / P_k)^{0,5} \quad (4)$$

where  $d$  is gas flow diameter at the crucible;  $P_j$  is flow cutoff pressure.

Figure 4 shows the diagram [11] which explains the tendency of local lead film thickness variations for different substrate lengths  $L$ , different ratios ( $P_j / P_k$ ) and different distances  $h$  to the substrate according to laser measurements. Flow expansion starts at the point where the flow sooner reaches the vacuum. If the crucible is mitered, there appears the pressure gradient deflecting vapor flow. Figure 5 shows lead film thickness variation for different crucible miters.

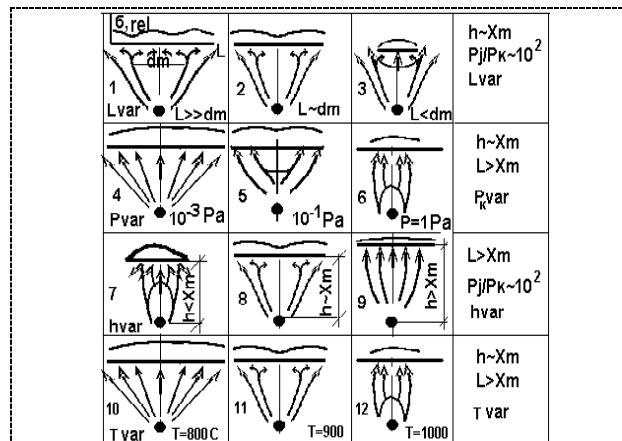


**Figure 4.** Vapor flow and substrate interaction diagram.

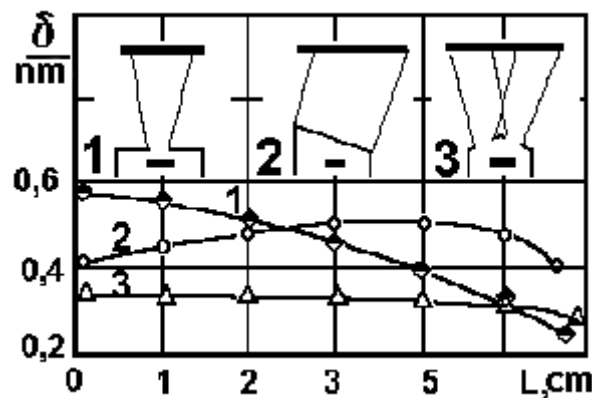


**Figure 5.** Film thickness distribution over the substrate for different miters.

4.1. *The influence of substrate.* Due to the holders, the picture of substrate  $L$  flow-around (1, 2, 3) even of small dimensions corresponds to the flow-around model of small infinite in size obstructions in transonic flow.

4.2. *The influence of chamber pressure.* As the chamber pressure reaches the evaporation pressure (4, 5, 6), the shape of flow effusion changes from sphere to torch, and agrees with Kneller diagram.

4.3. *The influence of distance.* As the substrate retreats from the evaporation cutoff (7, 8, 9), the vapor flow shape changes from the high-amplitude mode to free flow mode. The film thickness changes from cosine to more uniform one. The evaporation temperature change (10, 11, 12) is adequate to the evaporation cutoff pressure increase and ratio decrease.

4.4. *Parametric thickness synthesis law control.* Changing the local temperature at a certain point of crucible miter results in thermobaric effect at which temperature differential causes pressure differential, which also contribute to vapor flow deflection.

## 5. Results and conclusions

The experiments on formation of lead and zinc films demonstrated that the locally coldest parts of the substrate or chamber elements are preferred centers of film condensation. Zinc is a bright flash

evaporator. Vapors super cooling and their aggregating happen in the region between the evaporator and the substrate. Parametric estimations showed that the ratio of local zinc vapor pressure to vacuum chamber pressure is  $\sim 100$ , the rate coefficient is  $\sim 2$ , the temperature function  $(\lambda) = 0,2$  at the evaporation temperature 6000 C. It means that the flow temperature fell by a factor of 5. Microscopic study showed that at the variable condensation function the film gets the shape of cumulo nimbus.

According to mass spectroscopy, during film formation the intensity of hydro carbonic component increases by a factor of 1-2 from  $10^{-6}$  to  $10^{-5}$  Wt due to gas emission from heated elements. The direction of gas-phase reaction is estimated with respect to absorbed gas  $Q$  from vacuum chamber with the volume  $V$  in a time unit [12].

$$Q = V \frac{dP}{dt} \quad (5)$$

With the temperature increase, segregate makeup of near surface phase is arranged in the following order: hydride, oxide, carbide, and nitride. The flow rate change (achieved by the evaporation rate change and chamber vacuum level) results in density and temperature functions change. The amount of gas in films can be estimated from the evaporation pressure change and from the isobaric potential diagram change.

$$\Delta Z = -RT \ln P_i \quad (6)$$

where  $R$  is a universal gas constant.

Taking into account gas-dynamic functions (1) and (2) the isobaric potential is:

$$\Delta Z = f(R, T, P_i) = f(R, \tau(\lambda), \pi(\lambda)) \quad (7)$$

where  $\tau(\lambda), \pi(\lambda)$  are gas-dynamic functions of temperature and full pressure distribution.

As a result,

$$\Delta Z = -R\tau(\lambda) \cdot \tau(\lambda)^{k(k-1)} \approx -R\tau^2(\lambda) \quad (8)$$

That is, the decrease of isobaric potential is proportional to temperature change function squared. Using numeric values of temperature functions  $\tau(\lambda)$ , one can see the following: when the flow is static  $\lambda \rightarrow 0, \tau^2 = 1$  the isobaric potential ( $\Delta Z$ ) doesn't change. When the working flow is close to sound velocity  $\lambda \rightarrow 1, \tau^2 = 0,64, \Delta Z = 0,64$ ; where  $\lambda \rightarrow 2,5, \tau^2 \rightarrow 0, \Delta Z \rightarrow 0$ .

One can see that the flow rate variation results in the change of density and temperature functions, which is followed by phase diagram shift by the flow rate coefficient squared. Figure 6 shows the isobaric potential.

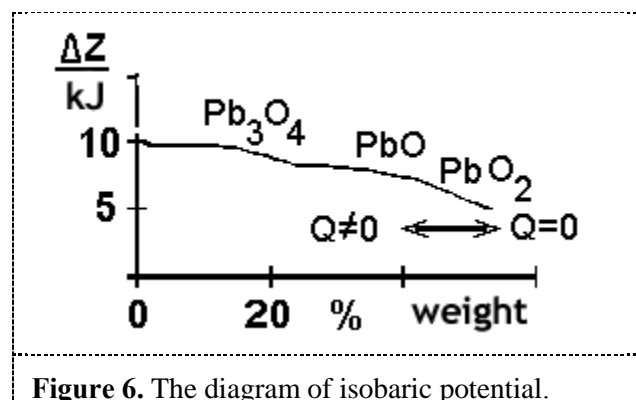


Figure 6. The diagram of isobaric potential.

The magnitude of isobaric potential and the percentage of absorbed gas at working gas inleakage decreases due to the decrease of local gas pressure.

## 6. Conclusion

According to gas dynamics laws we were able to find conditions which allow forecasting the rules of local optical layer thickness distribution and gas-phase reaction route at the minimal distance from the substrate to evaporator and maximal material utilization rate. The obtained results on geometric and parametric vapor flow control were used in formation of zinc oxide waveguides on glass substrate [13-14]. The dynamic approach enables to increase the uniformity of film thickness in the process of Gallium Arsenide molecular-beam epitaxy.

## Acknowledgements

This work was financially supported by The Ministry of Education and Science of the Russian Federation in part of the science activity program.

## References

- [1] Peitmann K, Hukriede J, Buse K and Kratzig E 2001 *Phys. Rev.* **61** 7 4615
- [2] Esseling M, Holtmann F, Woerdemann M and Denz C 2010 *Optics Express.* **18** 16 17404
- [3] Arestov S and Orlikov L 2013 *Izvestiya vuzov, ser. Fizika* **56** ½ 178-181
- [4] Makhov I., Makhova P., Pomazkova E 1990.– *Electron. Promyshl.* 1990, No 10, P.64-65.
- [5] Ohashi M, Ozeki M and Cui J 1999 *Rev. Sci. Instrum.* **85** 7522-27
- [6] Abramovichm G N 1976 *Prikladnaya gazovaya dinamika* Moscow Nayka 808
- [7] Zarvin A, Sharafutdinov R u.a 1979 *Diagnosis of rarefied flows gaza* Novosibirsk ITF 179-188
- [8] Vasenkov A, Sharafutdinov R, Belikov A and Kuznetsov O 1995 *Microelectronika* **24** 3 163-165
- [9] Neller G 1976 *Dynamic rarefied gas* editor A. Isclinski Moskau, Mir, 195-206
- [10] Kimura T 1977 *AIAA Journal* **5** 611-612.
- [11] Orlikov L and Orlikov N 2001 *Technical Physics Letters ZHTF* **27** 10 881-882
- [12] Rosanov L 1990 *Vacuumnaja Technica* Moskau 320
- [13] Orlikov N, Orlikov L and Shandarov S 2001 *Radiotekhnika i elektronika* **11** 112-115
- [14] Orlikov L N, Orlikov N L, Arestov S I, Mambetova K M and Shandarov S M 2015 *IOP Conf. Ser.: Mater. Sci. Eng.* **81** 012043